Tailoring plasmon resonances in metal nanospheres for optical diagnostics of molecules and cells

Krystyna Kolwas, Dr hab.
Prof. at the Institute of Physics, Polish Academy of Sciences,
Al. Lotników 32/46, Warszawa, Poland;

Anastasiya Derkachova, Dr
Institute of Physics, Polish Academy of Sciences,
Al. Lotników 32/46, Warszawa, Poland;

Daniel Jakubczyk, Dr
Institute of Physics, Polish Academy of Sciences,
Al. Lotników 32/46, Warszawa, Poland;

Content

Abstract

The advent of nanotechnology introduced a variety of novel exciting possibilities into diagnostic and sensing applications. Noble metal nanoparticles are of special relevance in that context, because their unusual properties fall mainly in visible, but also near-infrared and near-ultraviolet range, depending on the nanoparticle size and kind of a metal. Nanoparticles interact strongly with light via resonant excitation of localized surface plasmons (LSP), and so can act as efficient receiving or/and scattering optical nanoantennas. Resonant excitation of LSP give rise to a variety of effects, such as frequency dependent absorption and scattering (resulting in bright colours of colloids of nanoparticles) and electromagnetic near-field concentration and enhancement. An intense interest in noble-metal nanoparticles is driven by diverse applications in sensing, biomedical diagnostics and therapy, energy transport and conversion, novel spectroscopic and microscopic techniques, novel (meta-) materials and others.

Direct plasmon characterization versus size greatly facilitates the optimisation of plasmon parameters in diverse applications. Functional relationship of plasmon resonance frequencies and particle size provided in this chapter for gold and silver nanoparticles embedded in diverse dielectric media, gives an important practical tool for e.g. predicting spectral performance of single or colloidal nanoparticles, in estimation of the shift of plasmon resonance in colorimetric probes, or adjusting plasmon resonance frequency to the desired molecular transition. Other discussed factors are the maximal enhancement of the local electric near field and its spatial distribution. Predicting the distribution of the field around nanoparticles reveals regions of maximal electric field enhancement and dark areas, which are extremely unfavourable in the context of field enhancement.

1. INTRODUCTION

The advent of nanotechnology introduced variety of novel exciting possibilities into diagnostic and sensing applications. At the nanoscale, optical, electronic and chemical material properties are significantly different from those seen in bulk. The unique features of nanostructures make them attractive for a wide range of applications. The continuous development of the methodology of synthesis of metal nanoparticles (NPs) (examples in Section 4) and of the ability to control their properties by means of size, shape and composition has opened a variety of novel possibilities for molecular biology, medicine, physics and chemistry. An intense interest in noble-metal NPs shown by scientists from different domains and by engineers is driven by diverse applications of NPs in sensing, biomedical diagnostics and therapy, energy transport and conversion, novel spectroscopic and microscopic techniques, novel (meta)materials and others.

The physical and chemical elementary processes that are vital for life involve energy exchange in the electronvolt range. Visible and near-infrared optical excitations are used to

study such processes. Conventional optical investigation methods allow microscopic scale resolution in these spectral ranges. However, routine observation of sub-wavelength structures with optical microscopes is, according to Abbe's criterion (Born & Wolf 1999), limited to about half the wavelength of light, which is too large to resolve nanometre sized structures such as biomolecules or cell components. Application of plasmonic structures allows overcoming this limitation.

From the point of view of optical diagnostics, noble metal nanoparticles are especially interesting because of their unusual optical properties (see Section 2) which arise from their ability to resonate with the light field. Nanoparticles interact strongly with light via excitation of localized surface plasmon (LSP), (see Section 2.1 and 6.1) and so act as the efficient optical nanoantennas that can capture light (see e.g. (Stuart & Haes 2005) for review). Resonant excitation of LSP in nanoparticles give rise to a variety of effects, such as frequency dependent absorption and scattering which can be tuned by particle dimensions (Kreibig & Vollmer 1995), (Sönnichsen et al. 2002), (Kolwas et al. 2009),(Kolwas & Derkachova 2010). Another advantage is the near field concentration and enhancement which can be exploited for a variety of applications (see (Wang et al. 2011), (Quinten 2011), (Aslan et al. 2005b), (Willets & Van Duyne 2007) for reviews) such as surface-enhanced Raman scattering (SERS), high-resolution microscopy, solar cells, non-diffraction limited nanoscopic waveguides or nanophotonic devices.

Noble metal nanoparticles have proven to be useful for biological uses ((Aslan et al. 2005b), (Stuart & Haes 2005), (Lakowicz 2006), (Liao et al. 2006), (Schuller et al. 2010), (Willets & Van Duyne 2007), (Sardar et al. 2009), (Khlebtsov & Dykman 2010) for reviews). Possibility of tailoring LSP resonance frequency (Section 6 and 7) and particle absorbing and scattering properties (Section 5) is of fundamental importance to such applications. Another important advantage is the sensitivity of LSP resonance frequency to the changes in refractive index of the immediate environment. Plasmons and the resulting enhanced electric fields, confined in small region adjacent to metal NPs, are the bases of novel, exciting possibilities in optical diagnostics and sensing. Gold nanoparticles, being resistant to oxidation and photo bleaching, are highly potent optical probes, which can replace conventional organic dyes. Gold and silver nanoparticles are amenable to the attachment of biomolecules or ligands. Plasmonic probes making use of absorption and extinction spectra of noble-metal NPs are very attractive for their rapid, real-time performance and sensitivity. To date, most applications of gold colloids (Aslan & Geddes 2009) have been based on the monitoring of changes in their colour (Section 2.2) resulting from the spectral shift of plasmon resonance which manifests in the absorption or scattering spectra (Section 5). This has led to absorption based colloid proximity sensors for e.g. DNA, or antibodies ((Aslan et al. 2005b) and ref. therein). The aggregation of noble metal nanoparticles, which can be induced by specific bioaffinity reactions, became basis for the development of colorimetric detection of DNA hybridization immunoassays ((Aslan et al. 2004), (Stuart & Haes 2005) and ref. therein). The close proximity of plasmonic nanoparticles in an aggregate is known to result in a red-shifted LSP resonance, due to the near-field coupling. In Section 3, we give some examples of such applications.

Some applications of LSPs are based on properties of the LSP electric field associated with resonant excitation of plasmons. Others are due to the manner in which these resonances manifest in the light intensity spectra. Understanding the fundamentals of resonant interaction of light with plasmonic nanoparticles is essential for studying LSP properties and for their optimal use. Though the spectacular optical effects in metal nanoparticles are studied systematically since Faraday work (Faraday 1857), the understanding of plasmon basis seems to contain still some confusion. Plasmonic nanospheres represent the simplest and the most fundamental structures for studying the fundamentals of plasmon phenomena. Surface plasmons (Section 2.1) are collective surface charge density waves and the associated surface confined fields, which arise when the incoming light wave resonates with a nanoparticle. Mie theory (Born & Wolf 1999), (Bohren & Huffman 1983) (Section 5.2), delivers an indispensable formalism enabling to calculate electromagnetic (EM) fields in the near and far field regions around a spherical particle of chosen size as well as the resulting field intensities (irradiances) and the scattering, absorption and extinction spectra (Kolwas Derkachova & Shopa 2013). However, the peaks appearing in observed absorption or scattering spectra (Section 5) cannot be automatically ascribed to the positions of plasmon resonances. Such presupposition can affect optimisation of plasmon parameters for some application (Section 2). For example, the enhancement of electric field for Surface Enhanced Raman Scattering (SERS) (Section 3.1) requires different optimisation than colorimetric methods (Section 6 and 7) (which consist in enhancement of intensity of light at certain wavelengths).

The fascinating properties of noble metal nanospheres emerge when the frequency of the incident light wave coincides with the resonance frequency of the LSP modes (like in case of waves on a string). Plasmon resonance performance can be directly predicted by solving the eigenmode problem of a metal nanosphere, using the formalism of Mie theory (see Section 5.2) and realistic modelling of metal optical properties (see Section 5.1). Direct dependencies of plasmon resonance frequency and resonance spectral width and strength (defined by plasmon damping rates) versus particle size for Au and Ag NPs embedded in diverse dielectric media follow from the modelling (see Section 7.2). Such direct size dependence of LSP resonance frequencies and of corresponding plasmon damping rates make an important tool which allow optimization of plasmon properties for given application. In particular, they provide direct information on the size of gold or silver nanospheres, which must be used to optimise the local electric field enhancement (see Section 7.4 and 7.5) by adjusting plasmon resonance frequency to the desired molecular transition. Direct plasmon characterization versus size greatly facilitates the optimisation of plasmon parameters (see Section 6) by choice of appropriate type of metal and estimation of the shift of plasmon resonance frequency for nanoparticles used as colorimetric probes (see Section 3.4). Other factors, which can be optimised by the modelling, are the maximal enhancement of the electric near field (see Section 7.4) and its spatial distribution (see Section 7.4 and 7.5). Predicting the distribution of field around NP reveals regions of maximal electric field enhancement and dark areas on the nanoparticle surface, which are extremely unfavourable for the field enhancement.

Intense research efforts are still underway to exploit new applications of these particles. In view of low toxicity of gold and (functionalized) silver nanoparticles, the large scope of these applications suggests that noble metal nanoparticles form a whole class of highly promising nanomaterials for new biological and medical applications.

2. OPTICAL PROPERTIES OF METALS AT THE NANOSCALE: PLASMON RESONANCES

From everyday experience, we know that metals interact strongly with light. A mirror is the best example: mirrors are usually manufactured by applying a metal coating to the back surface of a substrate (glass) which makes them lustrous. The reason for this is so that metals have high density of freely moving electrons detached from their core atoms. These electrons screen the electric field of light at frequencies below the plasma frequency, causing reflection of light in visible range.

At the nanoscale, metal (in the form of a nanoparticle) possesses unique properties that are astonishingly different from those exhibited by metal in bulk. Nanometals exhibit striking reactive features, unusual electric conductivity and mechanical properties (including friction and ductility) and spectacular optical effects. The optical effects are the subject of our further interest.
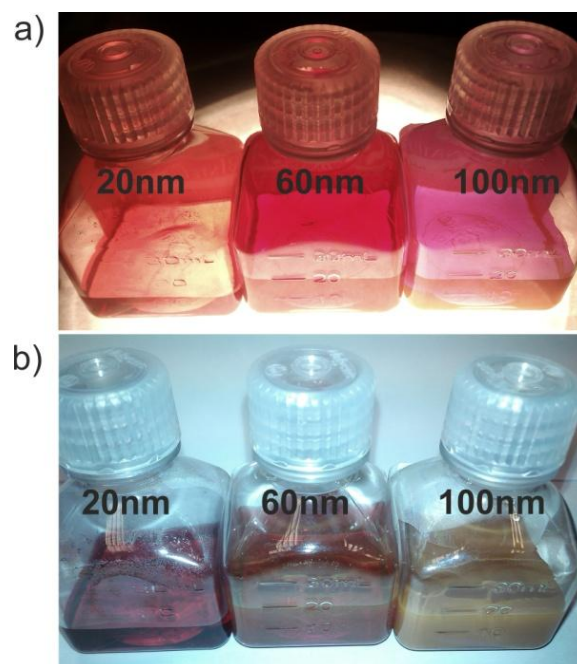
Figure 1. Suspensions of spherical gold particles with various diameters (20, 60 and 100 nm from right to left) in water. White light illumination from a) behind; b) from the front. The colour in a) is due to extinction, in b) due to diffuse back-scattering.

The resonance nanoscale optical effects, which can be observed even with a necked eye, are due to the strong interaction of light with the free-electrons of metal nanostructure. Gold, the element known as truly noble, can serve as an example. Gold, which is reduced in size to the

nanometre range, loses its well-known colour and changes it versus the nanoparticle size (see Figure 1).

Figure 2. Image of a sample containing gold and silver nanospheres as well as gold nanorods photographed with a dark field microscope (Sönnichsen 2001).

Figure 2 (Sönnichsen 2001) shows a true-colour image of a sample containing gold and silver nanospheres as well as gold nanorods observed wit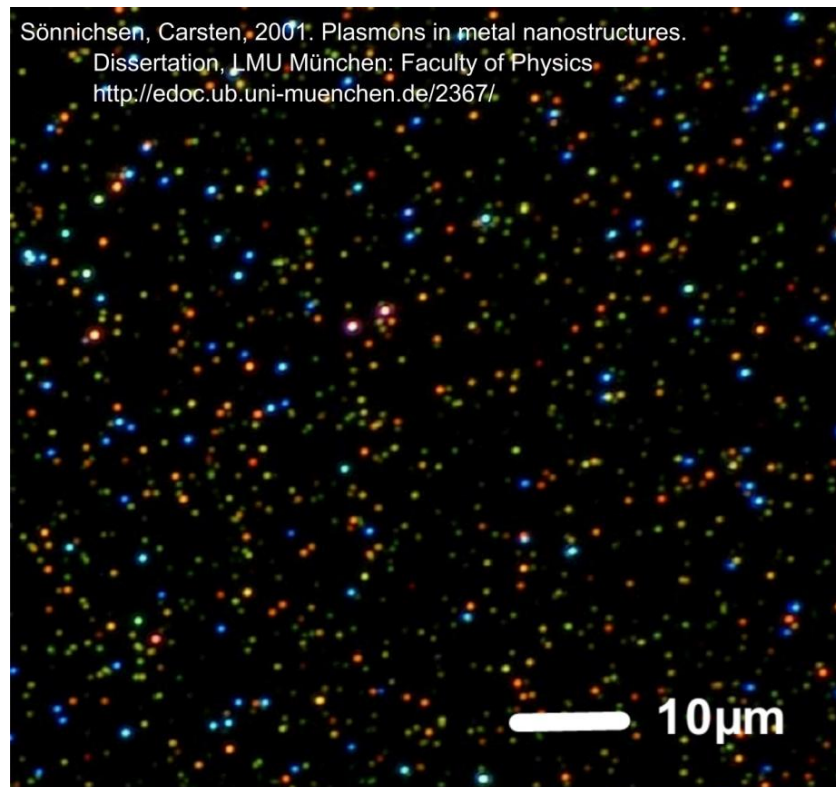h a dark field microscope. Each bright dot corresponds to an individual nanoparticle, which scatters light at a different plasmon resonance frequency. The resonance wavelength varies from blue (silver nanospheres) via green and yellow (gold nanospheres) to orange and red (nanorods).

Spectacular optical effects are born in the very proximity of nanometre-sized metal structures (in so-called near-field region), so they belong to the nanoworld. Technically 'nano' denotes one billionth of any fundamental unit, while nowadays 'nano' is used as an adjective to describe objects, systems, or phenomena with characteristics arising from nanometre-scale structure. Some of these effects can be observed by a far-away observer (in so-called far-field; at macro-dimensions) with a necked eye.

2.1. Localised surface plasmons

Spectacular colours of colloidal nanoparticles are due to resonant excitation of localized surface plasmons (LSP) (see e.g. (Maier & Atwater 2005), (Weiner 2009), (Dragoman & Dragoman 2008) for reviews): LSP are defined as collective oscillations of free-electrons at the metal-dielectric interface and the corresponding fields confined to the surface.

Spherical metal surfaces have an advantage, in contrast to infinite planar interfaces (e.g. (Maier & Atwater 2005), (Dragoman & Dragoman 2008)), of direct excitation of LSP by light. Surface plasmon propagating along an infinite planar metal surface (often called surface plasmon polariton (SPP)) can be excited only under the wave-vector selection rules (see e.g. (Dragoman & Dragoman 2008)), which limit direct coupling of SP with light. In contrast to SPP waves, LSP are standing waves and do not propagate. Thus, the term "localized" denotes plasmon standing waves on spherical metal/dielectric interface of a nanoparticle, which is comparable to, or smaller than the wavelength λ_{inc} of light used to excite the plasmon.
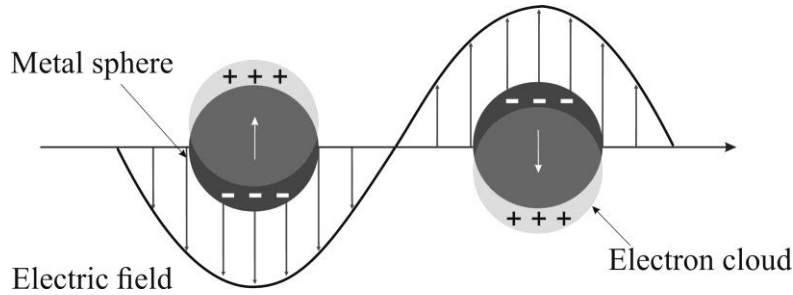

Figure 3. Schematic diagram illustrating a localized dipole surface plasmon.

Dipole surface plasmons in nanoparticles are usually imagined as back-and-forth normal-mode oscillations of the whole cloud of valence electrons, relative to the rigid, positively charged core (e.g. (Kreibig & Vollmer 1995), (Willets & Van Duyne 2007). In such a simplified picture, EM field of light drives the collective oscillations of nanoparticles free electrons (see Figure 3) at a certain resonance frequency, producing dipole charge density distribution near the surface. Subsequently, the oscillating electrons radiate EM field at the frequency of their oscillation. It is than elastic re-radiation of light with the same frequency.

However in reality, the radiating (scattering) abilities of nanoparticles change with particle size and are weaker for smaller nanoparticles, as discussed in detail in (Kolwas, K., Derkachova, A. & Shopa, M., 2009), (Kolwas, K. & Derkachova, A., 2010) and (Kolwas, K. & Derkachova, A., 2013). In general, excited collective charge density waves can be of dipole, quadrupole, hexapole (see Figure 4) or higher-polarity type, or can be a combination of multipoles, depending on the particle size. For increasing particle size, higher order plasmons can be effectively excited. Surface charge density waves of LSP are 3D standing waves, which, at the particle circumference, scale with the particle radius. Charge oscillations are coupled to the electric field confined to the surface and the field is strongly enhanced in respect to the incoming field (Section 7.4). LSP resonance occurs (Section 6) when the frequency of the incident EM wave fits to the resonance frequency of the allowed surface standing waves. Therefore, LSP waves can oscillate only at certain frequencies, which can be tailored by particle size and shape, type of a metal and of dielectric environment.
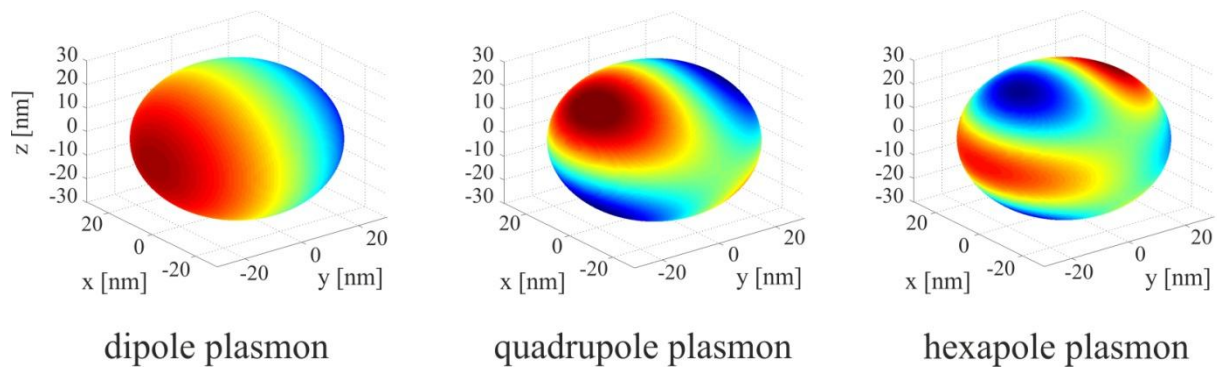
Figure 4. Examples of charge density distributions of the dipole, quadrupole and hexapole plasmon at the corresponding resonance frequencies. Illumination from the bottom with light polarized along x axis (see Figure 15a)). Red and blue regions represent maxima and minima of the surface electron densities.

Coherent surface charge oscillations at optical frequencies cannot be observed straightforwardly in any experiment. However, there is evidence of their existence in the near-field optical images (e.g. (Esteban et al. 2008), (Lin et al. 2010)). In principle, SPs are recognized for their intense electromagnetic fields bound to the surface. Therefore, the term "plasmons" refers (Dragoman & Dragoman 2008), (Sambles & Bradbery 1991), (Barnes et al. 2003), (Barnes 2006), (Zakharian et al. 2007), (Wang et al. 2011)], in practice, rather to light confined to the metal-dielectric interface. Their much-desired characteristics are shortened wavelength and enhanced field strength as well as sensitivity of LSP resonance frequency to changes in optical properties of the nanoparticles immediate environment.

2.2. Colour effects (far field)

Plasmon resonances manifest as the intense absorption or scattering of light, depending on the particle size (Section 5.2.1), and are the source of beautiful colours which has attracted the interest of artificers and scientists for generations.

The unique properties of nanoparticles were empirically known and utilised since ancient times for colouring ceramics and glasses. The Roman Lycurgus Cup (Figure 5) (now at the British Museum, London (Anon n.d.) represents one of the outstanding examples. Under normal lighting, this cup appears green. However, when illuminated from within, it turns to a glowing translucent red. The dichroic effect was achieved by adding tiny proportions of nanometre-sized alloy of silver and gold, which selectively absorbs some wavelengths, but reflects others.

In the Middle Ages, gold nanoparticles were used for manufacturing the stained-glass windows of Gothic churches. Stained-glass window makers achieved deep reds by dissolving gold in the molten glass. The stained-glass rose window at Notre Dame de Paris (Figure 6) makes a prominent example. When light shines through the glass containing gold nanoparticles, some wavelengths are absorbed within plasmonic mechanism, and others pass

Figure 5. The Roman Lycurgus Cup viewed in reflected (left) and transmitted (right) light. http://www.britishmuseum.org/explore/online_tours/museum_and_exhibition/the_art_of_glass/the_lycurgus_cup.aspx

through. Introducing different metals to the glass can alter its colour. Also, variation of the technological process, that modify the size (and shape) of the nanoparticles embedded in glass, leads to colour changes. Metal or metallic oxide nanoparticles are what actually give glass its colour: gold gives a deep ruby red; copper gives blue or green, iron gives green or brown, and so forth.
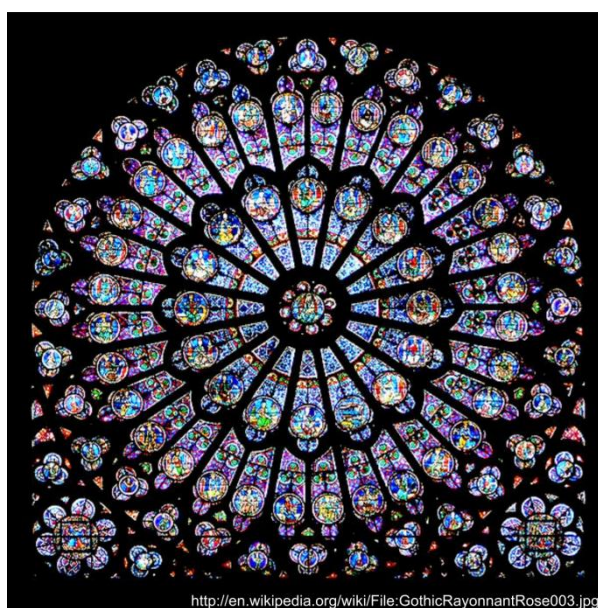
Figure 6. Gothic stained glass rose window of Notre-Dame de Paris. The colours were achieved by using colloids of nanoparticles.
http://en.wikipedia.org/wiki/File:GothicRayonnantRose003.jpg

However, the scientific research on nanogold seems to have started with Michael Faraday (Faraday 1857). Faraday reported that the mere variation in size of particles gave rise to a variety of resultant colours. Colloidal suspensions of nanospheres (see Figure 1) show bright colours, despite the extremely low concentration of gold particles (< 10−2 weight %). In

addition, the colours in the transmitted light are not a simple complement of the absorbed ones.

Contemporary scattering experiments allow observation of single metal nanoparticles under the dark-field microscopes (see Figure 2). The nanoparticles illuminated with white light appear to be of diverse colours depending on particle size and shape. Gold nanoparticles of a diameter of few tens of nanometres (see Figure 2) can be easily seen under a microscope using dark field condenser because of intense scattering with plasmonic mechanism (Jain et al. 2008), (Liao et al. 2006), (El-Sayed et al. 2005). The optical diameter of gold nanoparticles is several orders of magnitude larger than its physical diameter (see Section 5.2.1). Taking advantage of the strong LSPR scattering of gold and silver nanoparticles conjugated with specific targeting molecules, allows the molecule-specific imaging and diagnosis of diseases such as cancer (El-Sayed et al. 2005). An additional advantage is that the colours of nanoparticles do not photo-bleach or blink.

2.3. Enhancement of the electric field (near-field region)

Plasmonic nanoparticles can convert optical radiation into intense, localized EM field distributed near the particle surface. By squeezing light into sub-wavelength volumes, plasmonic structures have a profound effect on the efficiency of many optical processes, including light–matter interactions (Schuller et al. 2010). The nature of nanometallic light concentrators is distinct from the dielectric lenses used in conventional optics. Such lenses cannot focus light to spots less than about half the wavelength, due to the fundamental laws of diffraction. The ability of strong light concentration makes noble-metal nanoparticles a powerful tool for biological applications, including surface-enhanced Raman scattering (SERS) (see Section 3.1) and other surface-enhanced spectroscopic approaches. Plasmonic nanoparticles have been used to enhance the sensitivity of several spectroscopic measurement techniques including fluorescence, Raman scattering, and second harmonic generation. All these methods require optimisation of the near-field enhancement factor and of the extent of enhanced field. Such fine-tuning and control of plasmon characteristics is the main key in plasmonic applications and can be achieved by choosing proper nanoparticle parameters (Section 6).

3. APPLICATIONS (EXAMPLES)

Existing and proposed applications of plasmonic nanoparticles are numerous (e.g. (Stuart & Haes 2005), (Lakowicz 2006), (Liao et al. 2006), (Schuller et al. 2010), (Willets & Van Duyne 2007), (Sardar et al. 2009), (Khlebtsov & Dykman 2010) for reviews). Most applications involve imaging and specimen characterisation, however therapeutic applications are also proposed. Such applications rely on exceptional features of plasmonic nanoparticles. These are: enhancement of the electric filed in particle proximity, tunability of plasmon resonance frequency and of absorbing/scattering abilities of nanoparticles, sensitivity of

plasmon resonance frequency to the index of refraction of the environment and to the presence of interactions between nanoparticles In addition, plasmonic nanoparticles inherit an important feature common to all nanostructures: resistance to photo-bleaching. Furthermore, gold nanospheres are resistant to oxidation while being prone to bioconjugation and biomodification.

3.1. Surface Enhanced Raman Scattering

The prime example of plasmonic specimen characterisation technique is Surface Enhanced Raman Scattering Spectroscopy (SERS) (e.g. (Schuller et al. 2010), (Mahajan et al. 2010), (Wang et al. 2007)). It is based on the classical Raman spectroscopy (inelastic scattering of light), which enables probing the vibrational states of molecules.

Raman spectroscopy is commonly used to analyse a wide range of materials (gases, liquids and solids), including highly complex materials such as biological organisms and tissues. However, the extremely weak inelastic scattering intensities limit the applications of this technique. Surface Enhanced Raman Scattering has been used to overcome this limitation. SERS allows detecting trace amount of molecules, micro-organisms or living cells adsorbed at the surface of a metallic nanostructure (see Figure 7) illuminated at wavelength corresponding to the plasmon resonance frequency (see Section 6). Such detection is possible due to the localization of electromagnetic field and resulting substantial enhancement of the electric field near the plasmonic particle. With the enhancement of the field within plasmonic mechanism, the detection of single molecules adjacent to plasmonic nanoparticles becomes feasible.

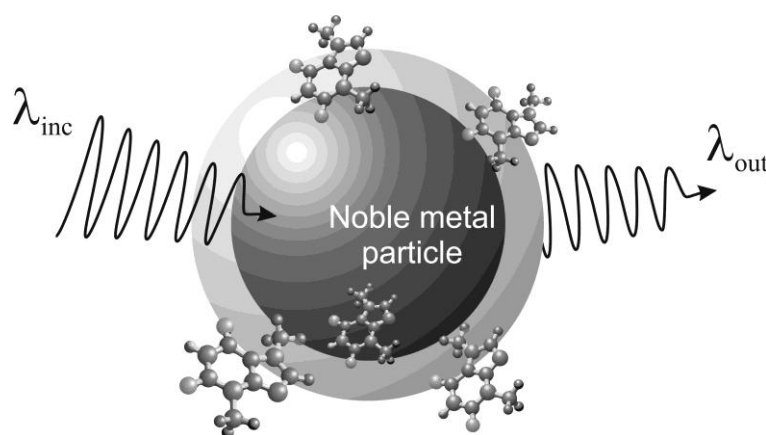**Figure 7.** Schematic drawing illustrating the interaction of molecules with the electric field enhanced in vicinity of a noble-metal nanosphere illuminated with light at plasmon resonance frequency. Non-resonant illumination of a molecule leads to the enhanced Raman emission, while illumination in resonance with absorption or emission band in a molecule can lead to plasmon-controlled fluorescence

3.2. Tissue markers

Since noble-metal nanoparticles are relatively biocompatible and nontoxic, plasmonic enhancement enables in vivo imaging of organisms and tissues. An important application is detection and diagnostics of specific tissues, such as tumours. when nanospheres are used as a contrast agent. Another example can be detection of specific micro-organisms/living cells adsorbed at the surface of nanospheres (see Figure 8, e.g. (El-Sayed et al. 2005), (Loo et al. 2005), (Chen et al. 2005), (Aslan et al. 2005b), (Jain et al. 2007), (Jain et al. 2008), (Khan et al. 2013)).
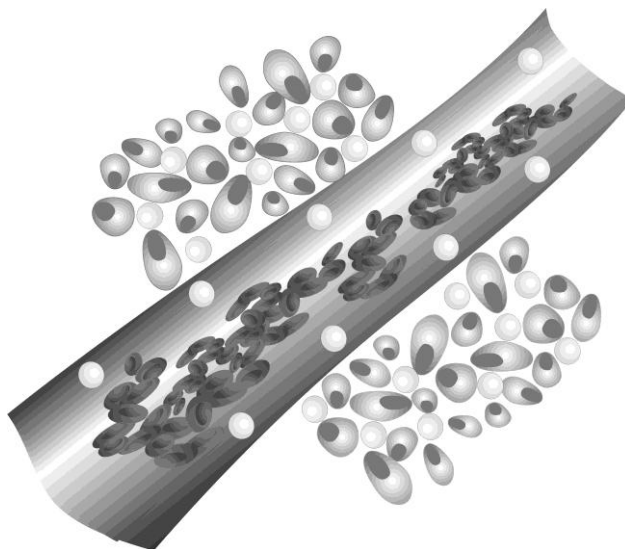

Figure 8. Gold nanospheres, which extravasate from the blood stream and accumulate in cancerous tissue due to the enhanced permeability and retention (EPR) effect, can be used as non-bleaching markers detectable with properly tuned light.

Gold nanoparticles in hydrogel polymer suspensions can be inserted by injection (see Figure 8). Long circulating gold nanoparticles extravasate from the blood stream and accumulate in tumour tissue due to the enhanced permeability and retention (EPR effect). The accumulated gold nanoparticles in cancerous tissue may be used as reference markers for precise localization of tumours in patients during radiation therapy, thereby improving treatment efficiency and reducing side effects due to irradiation of healthy tissue (El-Sayed et al. 2005).

Dark field microscopy enables observation of even single metal nanoparticles, and imaging of biological materials using metal nanoparticles as contrast agents. Dark field microscopy collects scattered light from a sample, whereas in typical transmittance mode microscopy, transmitted light is used to form images. Metal nanoparticles of proper (large enough, see Section 5.2.1 and 6.1) size show distinctly under dark-field microscopy because they can efficiently scatter incident light which is in resonance with their own plasmon resonance frequency. Then, even specimen regions with similar refractive indices can be distinguished (see Figure 9, (El-Sayed et al. 2005), see also (Wax & Sokolov 2009)).
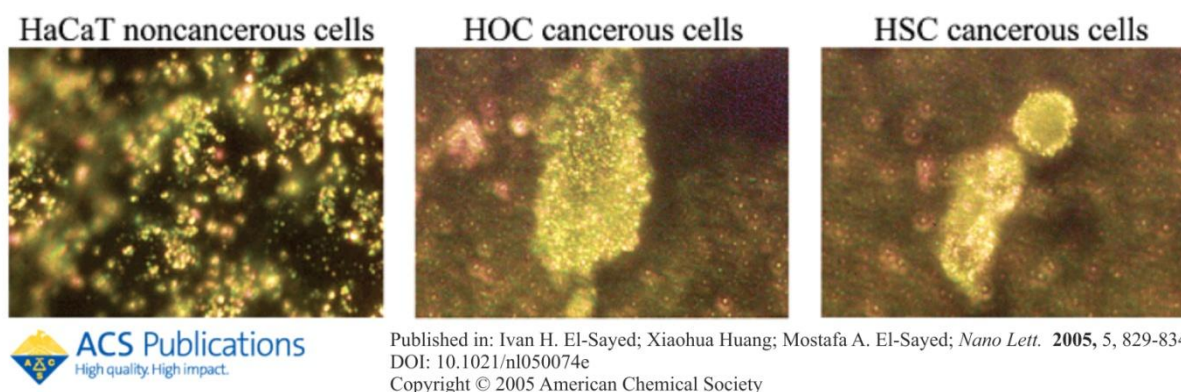
HaCaT noncancerous cells   HOC cancerous cells   HSC cancerous cells

Figure 9. Dark-field microscope images of specific-antibody-conjugated gold nanospheres used as contrast agent for cancer cell labelling (El-Sayed et al. 2005).

3.3. Plasmon-controlled fluorescence

Fluorescence detection is the basis of many measurement techniques in biological research (Lakowicz 2006). The sensitivity of fluorescence measurements largely determines progress in biology and medicine. A metallic nanoparticle can modify both the excitation and fluorescence of the molecule. Fluorophores situated in nanoparticle proximity can undergo near-field interactions with plasmonic nanoparticle and vice-versa. At very short distances, the nonradiative plasmon excitation decay dominates and the quantum efficiency of the emitter drops (Rogobete et al. 2007). Thus, the apparently very strong enhancements of the excitation field with plasmonic mechanism might not lead to a large enhancement of the molecular emission rate.

Such reciprocal interactions suggest that the novel optical absorption and scattering properties of metallic nanostructures can be used to control the decay rates, location, and direction of fluorophore emission. This opens way to ultra bright single-particle probes that do not photobleach, as well as to probes for selective excitation with decreased light intensities etc (see (Lakowicz 2006) for review).

3.4. Colorimetric detection

Colorimetric detection methods (Chen et al. 2013), (Gartia et al. 2013) are very attractive since they are rapid, sensitive, and real-time. Gold nanoparticles are very efficient colorimetric probes owing to their specific optical properties, which include modification of their plasmon resonance frequency by the index of refraction of the immediate environment, by increasing size resulting from nanoparticle aggregation or by the near-field interaction between nanoparticles.

The close proximity of two nanoparticles is known to result in a red-shift of plasmon resonance, due to near-field coupling. It can be directly utilised as a so called "plasmon ruler" (Reinhard et al. 2005), (Jain et al. 2007a) for measuring nanoscale distances between individual molecules. This feature can also be used in sensing techniques, based on looking

for changes in plasmon absorption. These changes are caused by the aggregation/di-sassociation of nanoparticles induced by the presence of a specific agent (detection of DNA damage (see Figure 10, (Chen et al. 2013)), protein conformational changes (Schneider et al. 2013) or heavy-metal ions contamination in water ((Pradeep 2009); see also (Aslan et al. 2005a)).
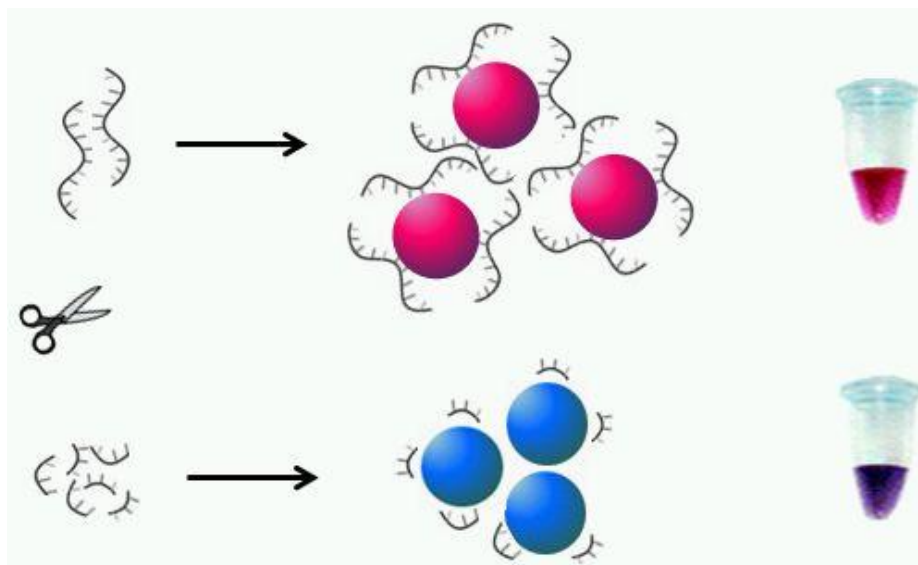

Figure 10. Binding of DNA fragments to gold nanospheres, influence their absorption spectrum due to the modification of the distance between spheres. The modification is characteristic to the fragment length. Thus the fragment length corresponds to characteristic colour of suspension and can be visually detected (Chen et al. 2013).

Functionalised noble-metal nanospheres can act as an assay (immunoassays, aptamer assays, etc.). Size-controlled nanosphere probes can be also used as suspensions exhibiting intense colours.

4. NANOPARTICLE SYNTHESIS (EXAMPLES)

With a large variety of potential nanoparticles applications, a large number of fabrication methods were devised to obtain desired particles controllably and reproducibly (see e.g. (Stuart & Haes 2005), (Khlebtsov et al. 2010), (Willets & Van Duyne 2007), (Shen et al. 2000), (Heiligtag & Niederberger 2013) for reviews). Gold and silver nanoparticles are commonly synthesized using reducing agents such as sodium citrate or sodium borohydride. Highly spherical gold and silver nanoparticles, without harsh reducing agents and with narrow size distribution are offered commercially by e.g. Sigma-Aldirich, nanoComposix, Cytodiagmostocs or mkNano. Two major groups of methods of nanoparticle synthesis can be distinguished: chemical wet synthesis and lithographic techniques.

4.1. Chemical wet synthesis

Chemical syntheses enable making particles of different shape (triangles, cubes, prisms, tetrahedra, bipyramids, and stars) and size. Though the particles morphology is (partially) controllable by the reaction conditions and the stabilising surfactant, the effects of polydispersity must be realised and accommodated.

In particular, metal nanoparticles of a variety of shapes and sizes can be produced by the reduction of a metal salt. Metal salts can be also reduced electrochemically in the presence of a surfactant or template. As far as colloidal Au is concerned, it seems that the most popular synthesis protocols involve the reduction of chloroauric acid (HAuCl4) by various reducing agents. For example, a very convenient citrate method (Turkevich et al. 1954), (Frens 1973), enables production of relatively mono-disperse particles with the controlled average equivolume diameter from 10 to 60 nm. However, for particles larger than 20 nm, the citrate method yields elongated particles (see e.g. (Brown et al. 2000)). Particles as small as 1 nm can be synthesised using sodium or potassium thiocyanate (Baschong et al. 1985) while only slightly larger (~5 nm) using sodium borohydride/ EDTA (Khlebtsov N. G. et al. 1996). Particularly promising spherical nanoparticles are those of a core-shell morphology. (Stuart & Haes 2005). Silica/gold (gold forming a shell) particles present an example of nanoparticles with spectral performance which can be tuned over 600–1500nm range by changing their ratio of the shell thickness to the core radius (Oldenburg et al. 1998),(Khlebtsov et al. 2010), (Yang et al. 2008), (Ye et al. 2009).

4.2. Lithographic techniques

This class of techniques yields substrate-bound nanostructures. Probably the most straightforward approach for making such structures is electron beam lithography (EBL). In EBL, first, the desired pattern is drawn with a high-energy electron beam on a thin layer of electron-resist, then the resist is chemically developed and the noble metal is deposited on the emerging structure. EBL provides very good control over the nanostructure morphology but is expensive and time-consuming.

An alternative set of methods for making surface-bound nanoparticle arrays is nanosphere lithography (NSL) and e.g. ((Haynes & Van Duyne 2001), (Haynes et al. 2002)). It is cheap and enables large-scale production, but the control over structure morphology is limited.

5. ABSORPTION, SCATTERING AND EXTINCTION OF NANOPARTICLES

Metal nanoparticles are known to both strongly absorb and scatter incident light, depending on their size, shape, refractive index of the dielectric environment as well as on the proximity to other resonant plasmonic nanostructures. The applicability of nanoparticles as contrast for biomedical imaging and as therapeutic agents relies on their spectral properties in the optical range of wavelengths. For instance, effective photothermal therapy with minimal laser

radiation dosage requires high nanoparticle absorption cross-section and low scattering losses. Contrary, cell imaging applications based on light-scattering microscopy require a high-scattering cross-section (Jain et al. 2006), (Jain et al. 2008). Transmission measurements directly yield the extinction of light, which consists of both absorption and scattering losses (Kreibig & Vollmer 1995). In case of small particles, scattering is negligible with respect to absorption, and the extinction can be directly assigned to the absorption cross-section.

If a colloid of such metal nanoparticles is illuminated by light of the frequency, which matches the plasmon resonance frequency characteristic for the nanoparticles size (Derkachova & Kolwas 2013), (Kolwas & Derkachova 2010), (Kolwas et al. 2009), absorption and/or scattering cross-section can be higher than the geometrical cross-section of nanoparticles. As compared to fluorophores, a 60 nm gold nanoparticle can produce the same scattering intensity as 3×10^5 fluorescing fluorescein molecules ((Aslan et al. 2005b) and ref. therein). The electrons in the metal nanoparticle exposed to the resonant electromagnetic wave can oscillate collectively at the same frequency as the incident wave. Collective oscillation of electrons and the associated EM fields are damped because of radiative and nonradiative processes. The contribution of each of them to the total oscillation damping rate is size dependent (Kolwas & Derkachova 2013). If the electron oscillation is damped mainly due to electron relaxation dissipative processes (the case of nanoparticles much smaller than the incident light wavelength), the absorption cross-section is large. With growing particle size, the oscillating electrons effectively re-radiate electro-magnetic radiation more effectively (see Section 6.1).

5.1. Description of material properties of metal nanoparticles

Realistic prediction of scattering and absorbing properties of single plasmonic nanoparticles or of their colloids is of crucial importance in applications. For this purpose, one needs a model describing both: the nanoparticle absorption and scattering spectra, as well as the intrinsic particle properties such as their plasmon resonance frequencies and plasmon damping rates versus size. However, numerical modelling leads to realistic predictions of these quantities only if realistic external parameters of the model are used. One of the crucial parameters is the frequency dependent complex refractive index of a metal nanoparticle $n_{in}(\omega)=n'(\omega)+i \cdot n''(\omega)$. It is related to the dielectric function of a metal nanoparticle $\varepsilon_{in}(\omega)$: $n_{in}(\omega)=\sqrt{\varepsilon_{in}(\omega)}$ which has to be supplied by an additional modelling. The recognition of the analytic form of $\varepsilon_{in}(\omega)$ enables the correct description of the dispersion of metal to the overall frequency dependence of absorption and scattering cross-sections as well as to the plasmon dispersion relation.

The simplest dielectric function often used to describe spectral properties of bulk metals is the Drude dielectric function. Drude model of a bulk metal treats free electrons as dimensionless negative charges forming homogeneous plasma uniformly distributed over the bulk and detached from the positively charged ions. In the framework of this model, when an external EM field of frequency ω is applied, the conduction electrons move freely between

independent collisions occurring at the average rate of γ. The frequency dependent dielectric function:

$$\varepsilon_D(\omega) = 1 - \frac{\omega_p^{\,2}}{\omega^2 + i\gamma\omega} \qquad (1)$$

explains the optical transparency of perfect metals ($\gamma=0$) observed above the plasma frequency ω_p (the index of refraction $n(\omega)$ is than imaginary). However, in many plasmonic applications of gold and silver nanoparticles, the function in such form is not satisfactory. The contribution of interband transitions to the optical properties of these metals makes them different from the perfect one. The simplest analytical function often used to describe spectral properties of real metals like gold or silver, results from the Drude-Lorentz-Sommerfeld model including the contribution of the interband electronic transitions accounted for as follows (Bohren & Huffman 1983):

$$\varepsilon_m(\omega) = \varepsilon_{ib} - \frac{\omega_p^{\,2}}{\omega^2 + i\gamma\omega}. \qquad (2)$$

ε_{ib} is the phenomenological parameter describing the contribution of bound electrons to the polarizability. If one adopts the effective parameters ω_p =9.01eV, ε_{ib} =9.84, and γ=0.072eV for gold and ω_p =9.10eV, ε_{ib} =3.7, γ=0.18eV for silver (Kolwas et al. 2009), (Derkachova & Kolwas 2013). $\varepsilon_m(\omega)$ reproduces the most widely used data sets of refraction indices for pure metals (Johnson & Christy 1972) quite well. The introduction of still another correction to γ over 1.8 eV range for gold enables even better modelling ((Derkachova & Kolwas 2014) to be published).

For a metal nanoparticle of size comparable to the electron mean free path in bulk (42 nm for gold), an additional relaxation mechanism arises due to collisions of electrons with the particle surface (see (Kreibig & Vollmer 1995), (Kolwas & Derkachova 2013) and references therein). This effect can be accounted by replacing γ in Eq. (2) with size dependent relaxation rate:

$$\gamma_R = \gamma_{bulk} + A\frac{v_F}{R}. \qquad (3)$$

v_F is the Fermi velocity, and A is the theory dependent quantity. In (Kolwas & Derkachova 2013) the accepted values are: A=0.33, $v_F = 1.4\times10^{-6}$ m/s for gold and A=2, $v_F = 1.4\times10^{-6}$ m/s for silver, and $\gamma_{bulk} = \gamma$ for the corresponding metal. Interface damping has little effect on the position of plasmon resonances in small nanoparticles. However, it has an important impact on the spectral width of plasmon resonance, which manifests in the absorption spectra of smaller particles. It also improves significantly the absorption abilities in comparison to the scattering capacities of nanoparticles of the same size. In all numerical simulations presented below, the dielectric function $\varepsilon_{in}(\omega)$ of a metal nanoparticle accounting for the interband transition and surface scattering effect with the effective parameters given above was used.

The optical properties of the nonabsorbing dielectric medium outside the sphere are usually independent on frequency in the optical range.

18

5.2. Rigorous Mie solutions

Mie scattering theory, which is more than a hundred years old, enables description of many spectacular effects described in Section 2. Mie solutions deliver indispensable formalism enabling to calculate EM fields in the near and far field regions around a spherical nanoparticle illuminated by light. Based on classical electrodynamics quantities, which are of experimental importance, can be found for chosen particle size and kind for diver optical properties of the environment. These are, for example, the intensities (irradiances) of elastically scattered light, as well as the spectra of absorption and extinction (absorption and scattering cross-sections, or absorption and scattering efficiencies). The calculated quantities are very close to the measured ones, if only the external parameters of the theory, such as the dielectric function of a metal or the refractive index of the environment are realistic (Section 5.1), and if the radius of the particle is well defined.

Mie theory considers a plane electromagnetic wave illuminating a spherical particle and the divergence-free Maxwell equations (with no external charge or current) supplemented by appropriate boundary conditions. The resulting Helmholtz equation for vector EM fields is solved in spherical coordinates. EM fields are expressed in the form of an infinite sum of partial electromagnetic waves of the "electric" (transverse magnetic (TM)) and "magnetic" (transverse electric (TE)) type, which are reciprocally orthogonal (Born & Wolf 1999), (Bohren & Huffman 1983). Mie theory supposes that the nanoparticles and the surrounding medium are homogeneous.

5.2.1. Absorption and scattering spectra of gold and silver nanoparticles

Spectral dependences of absorptive and scattering abilities of a nanosphere follow dependences of absorption and scattering cross-sections calculated on the basis of Mie theory for a particle of radius R embedded in a dielectric environment of the refractive index n_{out}.

Figure 11 a), b), shows the total absorption $C_{abs}(\lambda,R)$ and the scattering $C_{scat}(\lambda,R)$ cross-section for gold nanospheres of radii $R = 5$nm and $R=75$nm respectively. As shown in the figure, the optical properties of spherical gold nanoparticles are highly dependent on the nanoparticle radius. Smaller nanospheres primarily absorb light (with the absorption maximum near 520 nm, (Figure 11 a), dashed line), while larger nanospheres exhibit increased scattering (Figure 11 b), solid line). Small silver nanoparticles are much better absorbers than the gold ones (Figure 11 a) and c)). However, the absorption in small silver nanoparticles falls in the range of wavelength shorter than for the gold ones, which absorb light in the visible range.
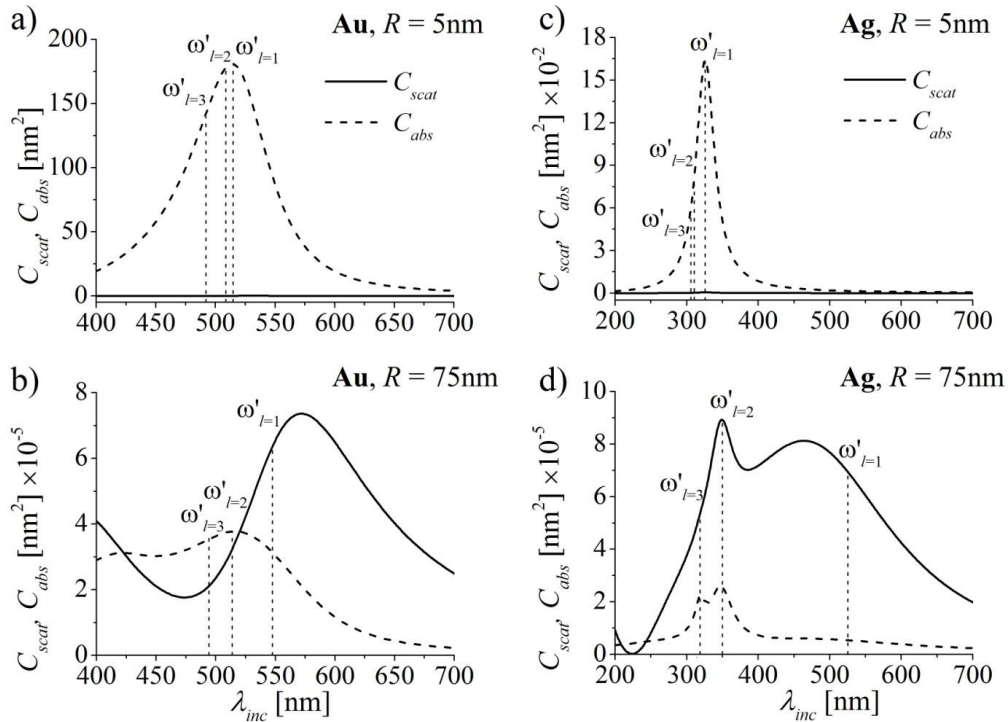
Figure 11. Absorption and scattering cross-sections of gold (a), b)) and silver (c), d)) nanoparticles of radius 5 and 75 nm respectively, $n_{out}=1$. Dashed vertical lines show the positions of surface plasmon resonances ($l = 1, 2, 3$ corresponds to the dipole, quadrupole and hexapole mode respectively, see Section 6.1) according to the solution of SP dispersion relation.

With increasing nanoparticle size, scattering maxima broaden significantly and shift towards longer wavelengths (red-shift). Larger nanospheres scatter much more light than the small ones. Absorption and scattering spectra of both small and large gold nanoparticles fall in the optical range (400-700 nm). It is worth noting that in the infrared spectral range, gold nanoparticles are not optically active, regardless of particle size. Absorption spectra of silver nanoparticles are shifted towards ultraviolet (see Figure 11 c),d)). However, large silver nanoparticles, which strongly absorb ultraviolet light, gain scattering abilities in the visible range, as shown in Figure 11 d). Thus, the increase of the scattering to absorption ratio with increasing size provides a tool for nanoparticle selection for contrast applications.

6. DIRECT SIZE CHARACTERISTICS OF SURFACE PLASMONS IN DIVERS ENVIRONMENTS

Mie scattering theory can correctly reproduce the positions of maxima in the observed spectra of a particle of a given radius. Maxima in the absorption or scattering spectra resulting from Mie theory are usually interpreted as the plasmon resonances. However, spectral positions of peaks in the scattering and absorption spectra are different and are size dependent, as demonstrated and discussed in Section 5.2.1 (see Figure 11) and in Section 6.2 below.

Therefore, the position of a maximum in the spectrum is not a perfect indication of LSP resonance condition. Moreover, Mie scattering theory is not a handy tool for determining the changes of the peaks in the spectrum due to the change of particle size. Effective controlling of spectral properties of plasmonic nanospheres is not possible without the knowledge about the direct dependence of LSP resonance frequencies and spectral widths (defined by plasmon damping rates) on particle size.

For simple geometries and sizes of the order of nanometres, the simplified theory predicts that the resonance frequency is independent of particle size (Kreibig & Vollmer 1995), (Schuller et al. 2010). Such approximation is valid when the size of a nanoarticle is significantly smaller than the free-space wavelength of the incident light λ_{inc}, so that the entire particle experiences uniform electric field at any time. Then, spherical nanoparticles exhibit the dipolar plasmon resonance at the frequencies $\omega = 2\pi c/\lambda_{inc}$, where $\varepsilon_{in}(\omega) = -2\varepsilon_{out}(\omega)$, and $\varepsilon_{in}(\omega)$ and $\varepsilon_{out}(\omega)$ are the dielectric functions of a metal nanoparticle and its dielectric environment, respectively, c is the velocity of light. When the nanoparticle size approaches the plasmon excitation wavelength, the optical phase varies across the particle and it is necessary to consider retardation effects. These inevitably lead to the dependence of plasmon resonance frequency versus size. Furthermore, not only the dipole plasmon but also higher order plasmons (quadrupole, hexapole and so on) come into play.

Tailoring of LSP properties by making use of the nanostructure size is a hot topic nowadays due to important applications in a variety of fields. Usually it is supposed, that prediction of plasmonic performance versus particle size is not possible within the rigorous modelling, since too many parameters must be taken into account including particle material, size and shape as well as optical properties of particle environment. However, for spherical particles it is feasible (Derkachova & Kolwas 2007), (Kolwas & Derkachova 2010), (Kolwas & Derkachova 2013), (Derkachova & Kolwas 2013). Absorbing and emitting optical properties of a spherical plasmonic nanoantenna can be described in terms of the size dependent resonance frequencies and damping rates of the dipole and higher order LSP. These quantities provide complete intrinsic LSP size characteristics. In (Kolwas & Derkachova 2010), (Kolwas & Derkachova 2013) such characteristics for gold and silver spherical particles were provided up to the large-size-retardation regime, where the plasmon radiative damping is significant. The size dependence of both: the multipolar LSP resonance frequencies and corresponding damping rates can serve as a convenient tool in tailoring the features of plasmonic nanoparticles in applications. Such characteristics enable to control the operation frequency of a plasmonic nanoantenna and to change the operation range from the spectrally broad to the spectrally narrow and vice versa. It is also possible to switch between particle receiving (enhanced absorption) and emitting (enhanced scattering) abilities. By changing the polarization geometry of observation (Demianiuk & Kolwas 2001), (Kolwas et al. 2009) it is possible to separate the dipole and the quadrupole plasmon radiation from all the non−plasmonic contributions to the scattered light.

Strict size characterization of LSP resonances of nanospheres of different metals embedded in diverse dielectric environments results from solving the eigenvalue problem (Kolwas & Derkachova 2013), (Derkachova & Kolwas 2007), (Kolwas & Derkachova 2010), (Derkachova & Kolwas 2013). In such description, spectrally selective optical effects are due to the elementary, intrinsic properties of a conducting spherical nanosphere embedded in a dielectric medium that can manifest in the optical response to the external electromagnetic field. The formalism of Mie scattering theory (Bohren & Huffman 1983) is used. However, while the intrinsic plasmonic properties of a nanosphere are studied, there is no illuminating field, as it is in standard formulation of Mie scattering theory. Only TM mode is considered. The dielectric function of a metal, being the external parameter of the modelling, is carefully chosen in order to represent the realistic optical properties of silver and gold (Johnson & Christy 1972) as a function of light wavelength. In addition, the surface electron scattering effect (Kreibig & Vollmer 1995), (Kolwas & Derkachova 2013) (also called the interface damping effect, (Section 5.1)) is taken into account. This effect causes the substantial modification of electron relaxation rates in particles of sizes comparable or smaller than the electron mean free path in metal. In gold nanoparticle, the additional correction to the electron damping rate above 1.8 eV is added in order to better reproduce the imaginary part of the dielectric function ((Derkachova & Kolwas 2014) to be published).

6.1. LSP resonance frequencies and damping rates as a function of size – results of rigorous modelling

Plasmon size characteristics result from considering the divergence-free Maxwell equations fulfilling continuity relations at the sphere boundary. Conditions for the existence of solutions, which are TM in character, correspond to complex frequencies of the fields. The real parts of these frequencies define frequencies of plasmon oscillation $\omega'_l(R)$ for a given mode l, ($l=1$ for the dipole plasmon, $l=2$ for the quadrupole plasmon and so on). Their imaginary parts $|\omega''_l(R)|$ define radiative damping rates (or equivalently: damping times) of plasmon oscillations.

Figure 12 illustrates LSP size characteristics of gold spheres in an environment of the index of refraction equal to 1.5 (e.g. the immersing oil). $\omega'_l(R)=\hbar\omega_l(R)$ and $|\omega''_l(R)|=\hbar/T_l(R)$, expressed in units of energy (electronvolts), describe size dependence of plasmon resonance frequency $\omega_l(R)$ and the damping time $T_l(R)$ (from the range of 1-20 fs) of LSP oscillations (Kolwas & Derkachova 2013). The dipole plasmon resonance frequency $\omega'_{l=1}(R)$ is a decreasing function of radius R. The same applies to the quadrupole ($l=2$) and higher multipolarity plasmon ($l>2$) frequencies, as illustrated in Figure 12 a). Plasmon resonance takes place, when the frequency of the incoming light wave fits to the frequency of plasmon mode in the particle of radius R: $\omega=\omega_l(R)$.
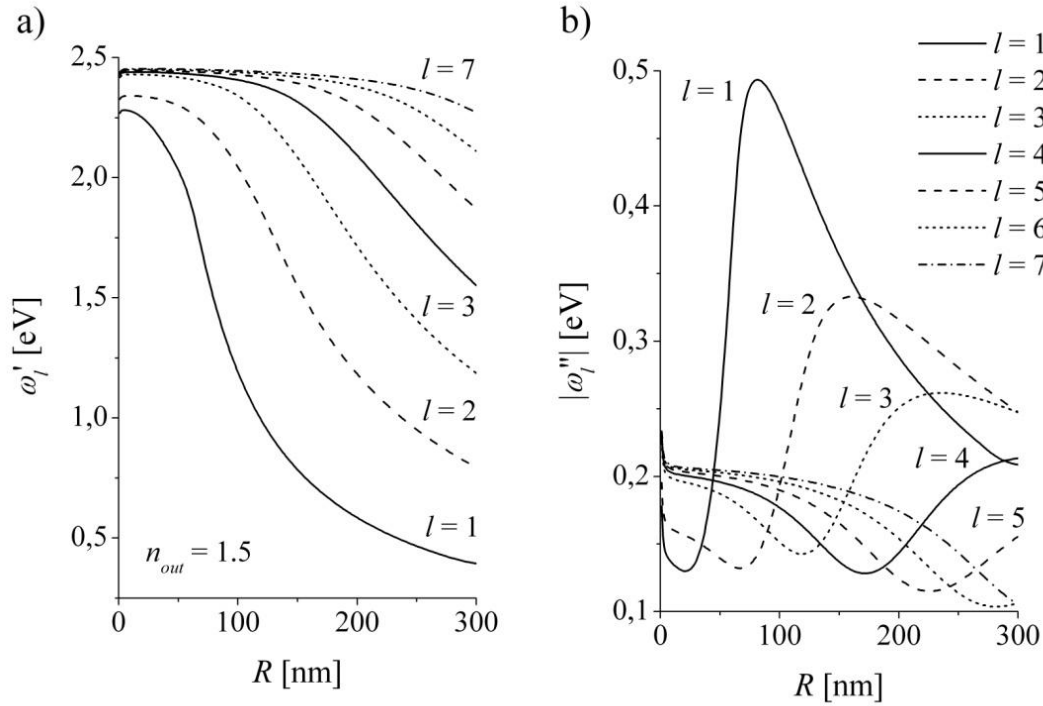
Figure 12. a) Multipolar plasmon resonance frequencies ω'_l and b) plasmon damping rates $|\omega''_l|$ versus particle radius R for n_{out}=1.5.

Plasmon oscillations are always damped due to the ohmic losses (absorption) and radiation of electromagnetic energy. With increasing particle size, the damping rate $|\omega''_l(R)|$ (see Figure 12 b)) is initially governed by the nonradiative damping resulting from electron collisions in a metal nanoparticle (see Eq. (3)); while for larger particles radiative damping is dominant. Particles of such size are good far-field scattering nanoantennas. Our study, extended toward large particle sizes and plasmon multipolarities, revealed new features of the total plasmon damping rates (Kolwas & Derkachova, 2013). In small nanoparticles, the total plasmon damping rate is close to the nonradiative damping rate resulting from absorption and heat dissipation while radiative losses are negligible. For larger particles, the suppression of nonradiative damping takes place when the radiative damping brings the dominant contribution to the total plasmon damping. That corresponds to the range of sizes for which $|\omega''_l(R)|$ is the fast increasing function of R (see Figure 12 b)). The reduction of nonradiative losses with the increasing contribution of radiation damping is revealed in the absorption spectra of particles; absorptive abilities of large particles are poor (Figure 11 b), d)).

Figure 13 a) and b) tells us what wavelength λ_{inc} of the incoming light should be used to excite dipole, quadrupole and hexapole plasmon resonances in gold nanoparticles of different radii and embedded in different environments: Figure 13 a) corresponds to air (n_{out}=1),and Figure 13 b) to water (n_{out}=1.3). Figure 13 c) and d) illustrate the corresponding dependencies for silver nanoparticles.
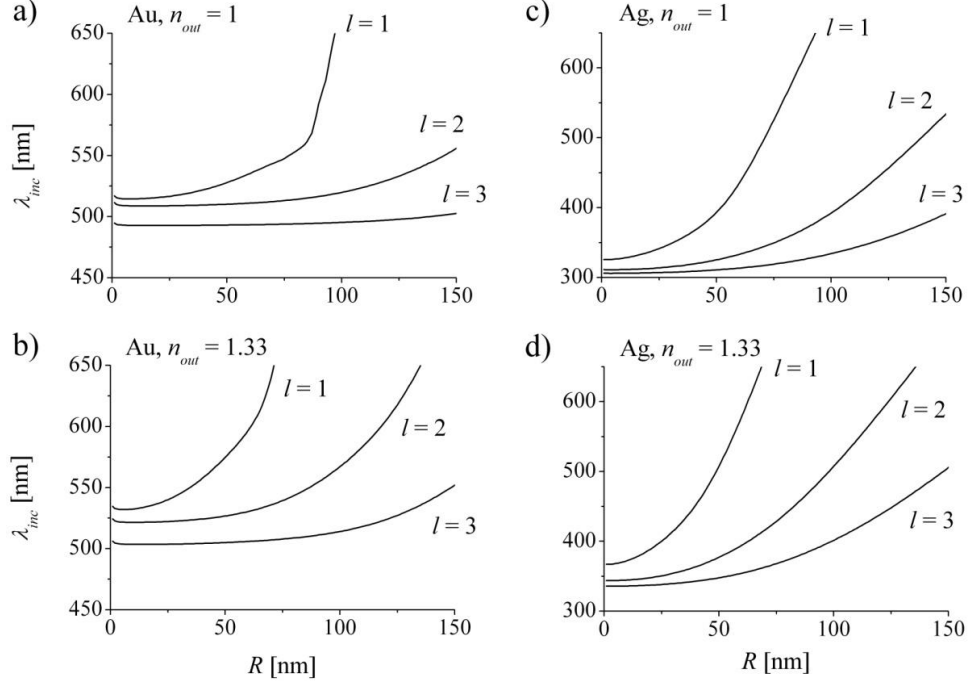
Figure 13. The wavelength of the incoming light field λ_{inc} corresponding to dipole ($l=1$), quadrupole ($l=2$) and hexapole ($l=3$) plasmon resonance frequency in gold (a), b)) and silver (c), d)) nanoparticles of different radii and in diverse environments: a), c) in air ($n_{out}=1$), and b), d) in water ($n_{out}=1.3$).

Figure 13 demonstrates that the frequency of plasmon oscillations in gold nanoparticles falls well into the visible range and is not very strong function of particle radius in large range of sizes. Resonance frequencies of the corresponding silver nanoparticles are strongly shifted toward shorter wavelength and for nanoparticles of smaller size fall into near UV range. Properties of silver nanoparticles are more sensitive to size then the corresponding gold nanoparticles.

6.2. Manifestation of LSP resonances in the absorption and scattering spectra

Maxima in the optical spectra of nanoparticles are manifestations of plasmon resonances at frequencies $\omega'_l(R)$ which in Figure 11 are marked with dotted vertical lines. However, the spectral positions of peaks occurring in the absorption spectrum (red line) and in the scattering spectrum (black line) are different.

In the absorption spectrum of small nanoparticles ($R=5$nm, dashed line in Figure 11), the maximum corresponds to the dipole plasmon resonance frequency $\omega'_{l=1}(R = 5\text{nm})$ for gold (Figure 11 a)), and for silver (Figure 11 c)) nanoparticles. However, for larger particles ($R=75$nm) (Figure 11 b) and d)), the manifestation of the dipole plasmon at $\omega'_{l=2}(R = 75\text{nm})$ in the absorption spectrum (dashed line) is suppressed (Kolwas & Derkachova 2013). Despite the dipole plasmon resonance frequency $\omega'_{l=1}(R = 5\text{nm})$ (marked with the corresponding horizontal line) is shifts towards larger wavelength (red-shift) with increasing particle size, the

absorption spectrum shifts toward shorter wavelengths (blue-shift). Though the dipole plasmon manifestation is suppressed in the absorption spectrum of small nanoparticles, in larger particles it participates in formation of the maximum in the scattering spectrum at the frequency $\omega'_{l=1}(R=75nm)$ marked by dotted vertical line in Figure 11 b) for gold and Figure 11 d) for silver nanoparticles. This can be explained by the increased contribution of the radiation damping to the total plasmon damping rate (Figure 12 b)) in larger particles. Higher order plasmons ($l>1$) are characterised by lower radiative damping rates for a particles of the same radii. Therefore, as long as the contribution of radiative damping of quadrupole and higher order plasmons is low, absorption in larger nanoparticles is not suppressed. As demonstrated in Figure 11 b), d), solid line), the position of the maximum in the scattering spectrum for larger particles is shifted in respect to the plasmon resonance position (Kolwas et al. 2009), (Kolwas & Derkachova 2013).

We can state, that in general, position of the maximum in the spectrum is not a perfect indication of the plasmon resonance in larger particles. However, the existence of such maxima can be used in applications, for example in the calorimetric techniques. With the increasing size of a particle, not only a substantial down-shift of plasmon frequencies (longer wavelengths), but also a significant broadening of the plasmon resonance take place (Sönnichsen et al. 2002), (Kolwas & Derkachova 2010), (Kolwas & Derkachova 2013). This feature can be predicted by our plasmon size characteristics (resonance frequencies $\omega'_l(R)$ and plasmon damping rates $|\omega''_l(R)|$ presented in Figure 12), which give the plasmon resonance position and the spectral width of plasmon resonance as a function of particle radius R. Despite the plasmon resonance in larger particles shifts toward longer wavelengths (see Figure 12 a)), the absorption spectrum shifts toward shorter wavelengths (see Figure 11 b) and d)) due to suppression of the absorptive particle abilities in the dipole mode. This refers to the existing controversy in interpretation of the observed plasmon optical properties. Modelling presented in this Section allows explaining the observed changes in spectral performance of metal nanoparticles as well as tailoring plasmon properties with understanding of the basis of the observed phenomena.

The interpretation of changes in colours of colloids, used in colorimetric detection (Section 3.4) of oxidative DNA damage caused by peroxynitrite (ONOO⁻) can serve as a practical example. The long single stranded DNA adsorbed onto gold nanoparticles prevents the aggregation of nanoparticles, and their optical response is the same as those of single, well separated nanoparticles with the dipole plasmon maximum in the red part of the spectrum (see Figure 11 a)). If DNAs are cleaved by ONOO⁻ to form small fragments, the gold nanoparticles aggregate forming large gold particles. One could expect, that due to the red-shift of plasmon resonance frequencies with increasing size (Figure 13 a) b)), the colour of the colloid will change toward the same spectral range. However, it is not the case. Large particles lose their absorbing abilities in the dipole mode due to the domination of radiative damping over all energy dissipation processes leading to absorption in nanoparticles (see the discussion above and Section 6.1). As the result, the spectrum is blue shifted, as confirmed by Figure 11 b), dotted line.

7. Optimization of plasmon features for diverse applications of nanoparticles: gold or silver?

Possibility of tailoring plasmon properties of nanostructures is the key to their applications and their development. Direct size dependencies of LSP resonance frequencies and of corresponding plasmon damping rates provide an important tool for optimization of plasmon properties in diverse application. Plasmon resonance frequencies, damping rates of plasmon oscillations and the number of plasmon modes l manifesting in optical spectra define the spectral performance of a plasmonic nanoparticle and can be controlled by the particle size, the type of metal and the optical properties of dielectric environment according to the model predictions (Section 6). The numerical tools based on electrodynamical description allow calculating the dependence of plasmon resonance frequencies and damping rates of plasmon oscillations (see Section 6.1) of metal nanoparticles embedded in diverse environments. The results of such modelling give direct information on the size of a gold or silver nanosphere which must be used to optimize the plasmon local electric field strength or scattered\absorbed light intensity spectra in the desired spectral range. Plasmon size characteristics help to decide what kind of metal nanoparticles should be used for a given application. Below we discuss the usefulness of the results of our modelling of plasmon features for optimisation of performance of plasmonic nanoparticles in diverse applications. We consider such features as: the shift of plasmon resonance frequency with size, the size dependence of nanoparticles absorbing and scattering abilities, the spectral sensitivity of plasmon features to the index of refraction of the environment, the strength of near-field enhancement, its spatial distribution and the extent of the plasmon enhanced field.

7.1. Size dependent plasmon resonance frequency

The explicit description of size dependence of plasmon resonances is very useful in numerous plasmon applications utilising e.g. the effective enhancement of the local near-field with plasmonic mechanism (e.g. in SERS (see Section 3.1)). If we intend to strengthen the fluorescence of the only few molecules which we have at our disposal, we should decide what size of plasmonic nanoparticle should be used in order to enhance the electric field around plasmonic nanoparticle. If, for instance, a molecular excitation wavelength $\lambda=514$nm, and we intend to use a gold nanoparticles, their radius should fall in the range up to 30 nm (in air) (as predicted by modelling, see Figure 13 a)). Such wide range of sizes makes using gold nanoparticles convenient. Moreover, the quadrupole plasmon frequency is in spectral proximity of the dipole plasmon, so we can expect excitation of both and thus an additional near-field enhancement. However, if gold nanoparticles are immersed in water, neither dipole nor quadrupole plasmon can be used for this purpose (see Figure 13 b)). What will happen if we replace gold by silver? In water, dipole plasmon resonance can be excited, but silver nanoparticle must be large, of radius larger than 50 nm (Figure 13 d)). Such large silver nanospheres are hardly available with the contemporary nanofabrication techniques.

7.2. Size dependent spectral absorbing and scattering abilities

The ratio of light scattering to light absorption can be tailored by the nanoparticle size (see Section 5.2.1, Figure 11). This provides a tool for nanoparticle selection for e.g. contrast agent applications. For instance, larger nanoparticles are more suitable for light-scattering-based imaging techniques, while smaller nanoparticles mainly absorb radiation and turn it into heat what can be of potential use in tumour therapy.

Changes in absorbing and scattering cross-sections with size can be explained by the size dependence of the total damping rates (Kolwas & Derkachova 2013) (see Section 6.1). If the dissipative, non-radiative damping contribution to the total damping rate prevails, absorption cross-section C_{abs} is large and scattering cross-section C_{scat} is negligible (see Figure 11). As long as the contribution of the radiative decay is negligible, the particle is not able to couple to the incoming light field effectively and has weak radiative (scattering) abilities. If the contribution of the radiative damping is large, the particle is able to emit light within plasmonic mechanism efficiently. Figure 12 b) gives an example of $|\omega''_l(R)|$ dependence for gold nanoparticles. This dependence allows distinguishing the size ranges in which efficient transfer of radiation energy into heat takes place (smaller nanoparticles) and those in which particles are good radiating antennas (larger nanoparticles with the fast increasing $|\omega''_l(R)|$ dependence).

Plasmonic absorption activity of silver nanoparticle falls in ultraviolet spectral range (see Figure 11 c),d)). However, by increasing particle size it is possible to make them plasmonically active also in the visible range, where their scattering cross-section C_{scat} (see Figure 11 d) is large.

Due to the plasmon enhancement mechanism, absorption and scattering cross-sections of gold and silver nanoparticles are significantly larger than their geometrical cross-section. These plasmonic particles are also superior to the absorbing and fluorescing dyes conventionally used in biological and biomedical imaging (Jain et al. 2006), (Jain et al. 2008). Note that in the infrared region gold and silver nanoparticles are optically inactive, regardless to particle size. Therefore they are not able to enhance the infrared radiation (e.g. in cancer therapy), as sometimes expected. However, properly designed gold nanoshell particles are used in experimenting with photothermal tumour therapy (Loo et al. 2005), (Gobin et al. 2007).

7.3. Sensibility to the index of refraction of the environment

An important advantage of LSP is the sensitivity of plasmon resonance frequency to changes in the refractive index of the immediate environment. Thereby, noble-metal nanospheres can act as efficient contrast agents (see Section 3.2).

The explicit size dependence of LSP resonance frequencies of nanoparticle in diverse environment is presented in Figure 14 a) for the dipole and in Figure 14 b) for the quadrupole

LSP of gold and silver nanoparticles correspondingly. The dipole LSP resonance frequency $\omega'_{l=1}(R)$ of both silver and gold nanoparticles exhibits a shift towards lower frequencies (longer wavelengths) with the increasing index of refraction n_{out} of the environment (see Figure 14 a)). Up to about 100 nm, plasmon resonance frequency of silver nanoparticles is much more sensitive to changes in optical properties of particle environment than that of gold. Therefore silver nanoparticles are more suitable in such applications as plasmonic biosensors. However, their plasmonic activity falls in UV. A similar conclusion can be drawn from the size dependence of the quadrupole resonance frequency, illustrated in Figure 14 b). For very large nanoparticles $\omega'_l(R)$ for gold and silver is similar when embedded in the same environment.
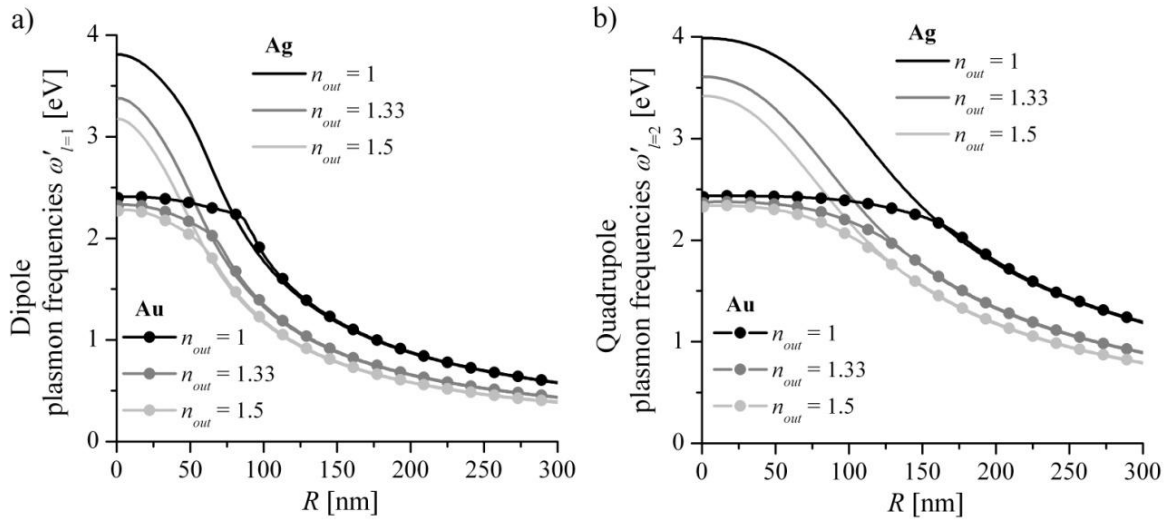

Figure 14. Dipole and b) quadrupole resonance frequencies as the functions of radius for silver and gold nanoparticles in air (n_{out}=1), water (n_{out}=1.33), and immersion oil (n_{out}=1.5).

7.4. The electric near-field strength and spatial distribution

Plasmon collective charge oscillations are coupled to the electric fields on (and near) the nanoparticle surface. These surface confined fields are strongly enhanced in respect to the incoming field of the light wave. The enhancement factor is not uniform in space and time. Its maximal value changes with particle size and for metal nanoparticles (if realistic modelling of their material properties is used) the enhancement is not largest for the smallest nanoparticles.

An important optimization factor results from the spatial distribution of total electric near field strength around the nanosphere. The local enhancement factor $\eta(R,\theta,\varphi,t)$ of the incoming electric wave with the amplitude E_0 is:

$$\eta(R,\theta,\varphi,t) = |\mathbf{E}^{out}(R,\theta,\varphi,t)|/E_0, \tag{4}$$

where $|\mathbf{E}^{out}| = |\mathbf{E}^{inc} + \mathbf{E}^{scat}|$ is the strength of the total electric field at the particle surface, illuminated by the incoming plane wave $\mathbf{E}^{inc}$, (r, θ, φ) are spherical coordinates (see Figure 15 a)).
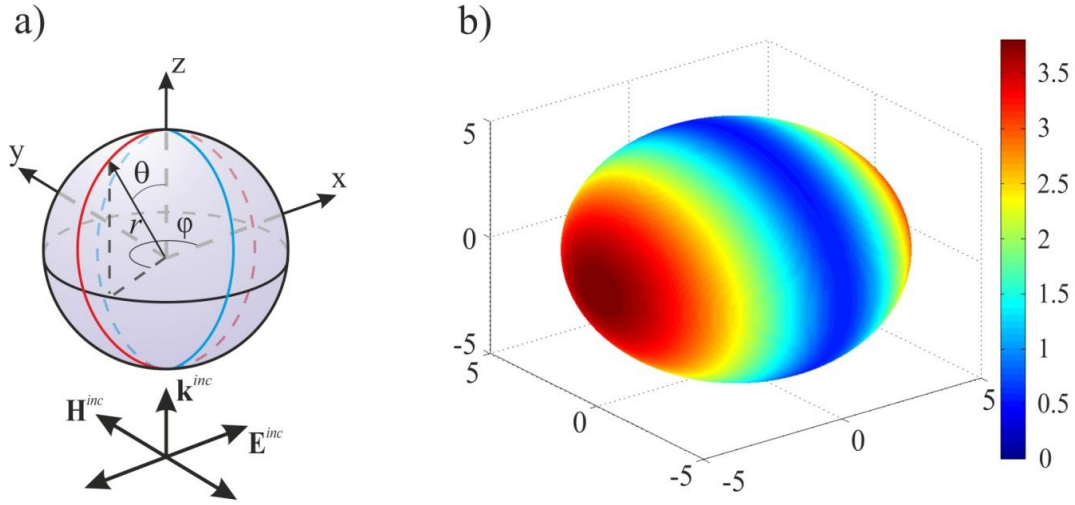

Figure 15. a) A scheme of plasmon excitation. b) 3D image of the enhancement factor $\eta(R, \theta, \varphi, t)$, for the dipole plasmon resonance frequency $\omega'_{l=1}(R=5\text{nm})$.

Spatial distribution of the enhancement factor displays a characteristic dynamic pattern, which follows the temporal dependence of the incident field. Analysis of the distribution pattern of $|\mathbf{E}^{out}(R, \theta, \varphi, t)|$ field allows distinguishing these areas on (or near) the nanoparticle surfaces, which are the most favourable for the electric field enhancement, and those which should be avoided. Figure 15 a), red circle, shows the favourable regions lying in the plane parallel to the plane of incidence on the meridian circumference. Exceptions are the south and north poles of a nanosphere, which are dark. The plane of incidence is defined by the polarization and the propagation direction of the incident light. The dark locations (dark blue colour) and the locations of maximally enhanced field (red brown) are presented in Figure 15 b). If used e.g. in SERS application (see Section 3.1), the molecules adjacent to the nanoparticle dark regions will not be excited at all; they will be totally lost from detection.

The maximal enhancement factor of small gold nanoparticles is lower than that of larger particles (Figure 16). It is partially due to the enhanced electron relaxation γ_R (see eq. (3) in Section 5.1) in small nanoparticles, which increases the absorption of light by a nanoparticle. Also, while smaller particles are not good scattering nanoantennas (see Section 5.2.1.) the strength of the total near field, must be smaller than for larger particles, as the numerical model simulations prove.
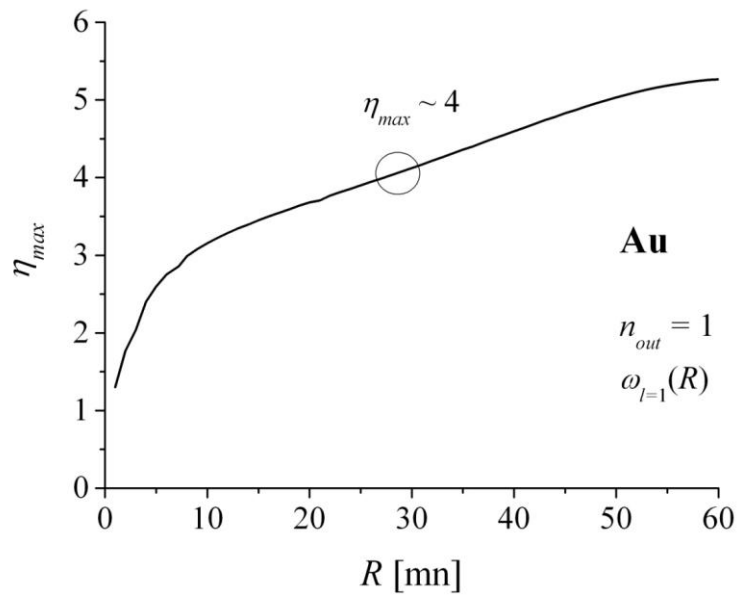
Figure16. Maximal enhancement factor η_{max} of the near electric near-field strength versus radius at the dipole resonance frequency of gold nanoparticle.

7.5. Extent of the plasmon enhanced field

Plasmonic nanoparticles are of particular interest in biological applications because they are of the same scale size as biological macromolecules, proteins and nucleic acids. Plasmon enhanced electric fields are known to be strongly localized near the surface. The extent of the enhanced near field around a plasmonic particle plays crucial role in applications. The penetration depth of the field into the particle environment should be in reasonable relation with the size of the object adjacent to the particle, and subjected to interaction with the field enhanced within plasmonic mechanism.

Figure 17 illustrates the maximal enhancement factor η_{max} versus distance d_0 form the surface of gold nanoparticles of diverse radii (R=10, 30 and 100 nm) at the corresponding dipole resonance frequency $\omega'_{l=1}(R)$. In larger nanoparticles, there is more room on the particle surface, and the maximal enhancement is not smaller. Therefore, it is worth to consider the extent of the enhanced plasmon field around a nanoparticle in comparison with the size of the studied object, which can be the atom, molecule or bacteria, in order to optimise their relative relation.
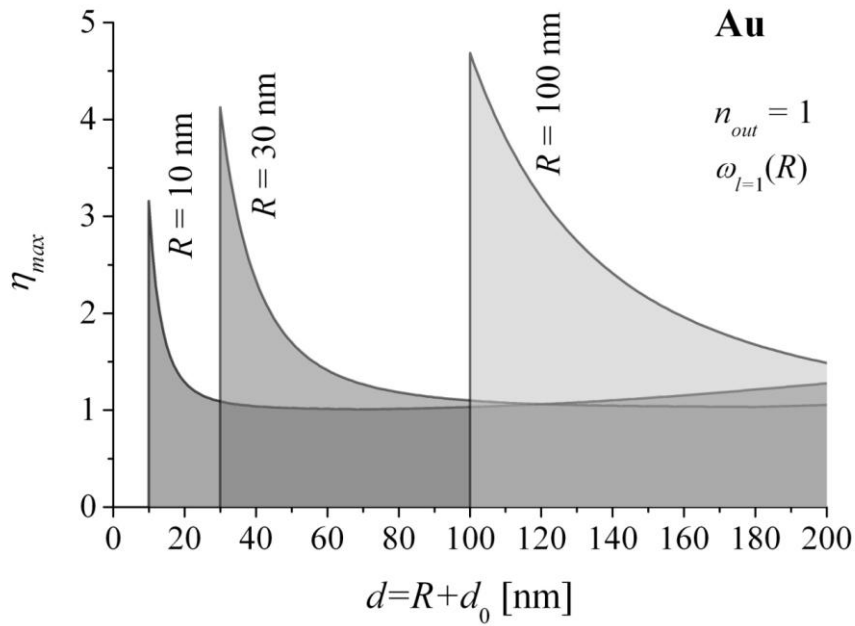
Figure 17. Maximal enhancement factor η_{max} for the dipole resonance frequency versus distance d_0 form the surface of a gold nanoparticle of diverse radii.

8. SUMMARY AND CONCLUSIONS

The main aim of the paper was to present some practical tools for tailoring plasmon characteristics to improve the optical diagnostics of molecules and cells, as seen by physicists. In the introductory chapters (Sections 1-4) we review those features of metals at the nanoscale which make them suitable in applications. These exceptional features result from ability of metal nanoparticles to resonate with electromagnetic radiation in the optical range, which leads to excitation of localized surface plasmon waves. Plasmonic nanoparticles can convert optical radiation into intense, localized EM field distributed near the particle surface. By squeezing light into a sub-wavelength volume in particle proximity, plasmonic structures have a profound effect on the efficiency of many optical processes being the basis of numerous applications. Some of them are reviewed in the introductory chapters. Plasmon resonances manifest as the intense absorption or scattering of light, depending on the particle size, shape and optical properties of particle environment. The sensitivity of plasmon resonances to these parameters is the basis of colour effects, constituting a large group of colorimetric detection methods. We do not pretend to make a full survey of applications of nanoparticles in biology and medicine. A choice of examples of the optical applications of plasmons is expected to point to further possibilities.

In Sections 5-7 we present a review of practical tools for tailoring plasmon characteristics to improve the optical diagnostics of molecules and cells. As we believe, improvement in applications is possible only, if the physical basis of the phenomena involved is well understood. Fundamentals of resonant interaction of light with plasmonic nanoparticles are

essential for studying LSP properties and for their optimal use. Practically, optimisation is possible, if one has the information concerning how the plasmon properties can be conveniently tailored, which parameters should be optimised and according to which formula it should be done. The presented study, which is an original contribution to the domain of physics of metal nanoparticles, delivers direct modelling of plasmon parameters as a function of nanosphere size, kind of metal used (gold and silver) and index of refraction of the particle environment. Language of classical electrodynamics was used and the appropriate solutions of Maxwell equations were found. Using the obtained plasmon characteristics it is possible e.g. to predict the spectral performance of colloids and explain the observed colours and interpret their changes. In addition, it is possible to control the changes in performance of plasmonic nanoantenna from good absorbing to good scattering device, and to optimise its near-field strength, spatial field distribution and extent of the plasmon-enhanced field. We hope that such study can be useful to a broad scientific community.

Acknowledgements

BIBLIOGRAPHY

Anon, The Lycurgus Cup. Available at: http://www.britishmuseum.org/explore/online_tours/museum_and_exhibition/the_art_of_ glass/the_lycurgus_cup.aspx.

Aslan, K. & Geddes, C.D., 2009. Wavelength-Ratiometric Plasmon Light Scattering-Based Immunoassays. Plasmonics, 4(4), pp.267–272.

Aslan, K., Lakowicz, J.R. & Geddes, C.D., 2005a. Nanogold Plasmon Resonance-Based Glucose absorption bands due to electron oscillations induced by. Anal. Chem., 77(7), pp.2007–2014.

Aslan, K., Lakowicz, J.R. & Geddes, C.D., 2005b. Plasmon light scattering in biology and medicine: new sensing approaches, visions and perspectives. Current opinion in chemical biology, 9(5), pp.538–544.

Aslan, K., Lakowicz, J.R. & Geddes, C.D., 2004. Nanogold-plasmon-resonance-based glucose sensing. Analytical biochemistry, 330(1), pp.145–155.

Barnes, W., Dereux, A. & Ebbesen, T., 2003. Surface plasmon subwavelength optics. Nature, 424(August), pp.824–830.

Barnes, W.L., 2006. Surface plasmon–polariton length scales: a route to sub-wavelength optics. Journal of Optics A: Pure and Applied Optics, 8(4), pp.S87–S93.

Baschong, W., Lucocq, J.M. & Roth, J., 1985. "Thiocyanate gold": small (2-3 nm) colloidal gold affinity cytochemical labeling in electron microscopy. Histochemistry, 83, pp.409–411.

Bohren, C.F. & Huffman, D.R., 1983. Absorption and scattering of light by small particles, Wiley.

Born, M. & Wolf, E., 1999. Principles of Optics, Cambridge University Press.

Brown, K.R., Walter, D.G. & Natan, M.J., 2000. Seeding of Colloidal Au Nanoparticle Solutions. 2. Improved Control of Particle Size and Shape. Chem. Mater., 12(2), pp.306–313.

Chen, J. et al., 2005. Gold nanocages: bioconjugation and their potential use as optical imaging contrast agents. Nano letters, 5(3), pp.473–477.

Chen, L. et al., 2013. Colorimetric detection of peroxynitrite-induced DNA damage using gold nanoparticles, and on the scavenging effects of antioxidants. Microchimica Acta, 180(7-8), pp.573–580.

Demianiuk, S. & Kolwas, K., 2001. Dynamics of spontaneous growth of light-induced sodium droplets from the vapour phase. Journal of Physics B: Atomic, Molecular and Optical Physics, 4075(01), pp.1651–1671.

Derkachova, A. & Kolwas, K., 2014, *to be published.*

Derkachova, A. & Kolwas, K., 2013. Simple analytic tool for spectral control of the dipole plasmon resonance frequency of gold and silver nanoparticles. Photonics Letters of Poland, 5(2), pp.69–71.

Derkachova, A. & Kolwas, K., 2007. Size dependence of multipolar plasmon resonance frequencies and damping rates in simple metal spherical nanoparticles. The European Physical Journal Special Topics, 144(1), pp.93–99.

Dragoman, M. & Dragoman, D., 2008. Plasmonics: Applications to nanoscale terahertz and optical devices. Progress in Quantum Electronics, 32(1), pp.1–41.

El-Sayed, I. H.; Huang, X.; El-Sayed, M. A., 2005. Surface Plasmon Resonance Scattering and Absorption of Anti-EGFR Antibody Conjugated Gold Nanoparticles in Cancer Diagnostics: Applications in Oral Cancer. Nano Lett., 5, pp.829–834.

Esteban, R. et al., 2008. Direct near-field optical imaging of higher order plasmonic resonances. Nano letters, 8(10), pp.3155–3159.

Faraday, M., 1857. The Bakerian lecture: experimental relations of gold (and other metals) to light. Philosophical Transactions of the Royal Society of London, 147, pp.145–181.

Frens, G., 1973. Controlled nucleation for the regulation of the particle size in monodisperse gold suspensions. Nature Phys. Sci., 241, pp.20–22.

Gartia, M.R. et al., 2013. Colorimetric Plasmon Resonance Imaging Using Nano Lycurgus Cup Arrays. Advanced Optical Materials, 1(1), pp.68–76.

Gobin, A.M. et al., 2007. Near-infrared resonant nanoshells for combined optical imaging and photothermal cancer therapy. Nano letters, 7(7), pp.1929–1934.

Haynes, C.L. et al., 2002. Angle-resolved nanosphere lithography: manipulation of nanoparticle size, shape, and interparticle spacing. J. Phys. Chem. B, 106(8), pp.1898–1902.

Haynes, C.L. & Van Duyne, R.P., 2001. Nanosphere lithography: a versatile nanofabrication tool for studies of size-dependent nanoparticle optics. J. Phys. Chem. B, 105, pp.5599–5611.

Heiligtag, F. & Niederberger, M., 2013. The fascinating world of nanoparticle research. Materials Today, 16(7/8), pp.262–271.

Jain, P.K., El-Sayed, I. & El-Sayed, M., 2007. Au nanoparticles target cancer. nanotoday, 2(1), pp.18–29.

Jain, P. K. et al. 2007a. On the Universal Scaling Behavior of the Distance Decay of Plasmon Coupling in Metal Nanoparticle Pairs: A Plasmon Ruler Equation. Nano Letters, 7(7), pp. 2080–2088.

Jain, P.K. et al., 2006. Calculated absorption and scattering properties of gold nanoparticles of different size, shape, and composition: applications in biological imaging and biomedicine. J. Phys. Chem. B, 110(14), pp.7238–7248.

Jain, P.K. et al., 2008. Noble metals on the nanoscale: optical and photothermal properties and some applications in imaging, sensing, biology, and medicine. Accounts of chemical research, 41(12), pp.1578–1586.

Johnson, P.B. & Christy, R.W., 1972. Optical Constants of the Noble Metals. Phys. Rev. B, 6(12), pp.4370–4379.

Khan, M.S., Vishakante, G.D. & Siddaramaiah H, 2013. Gold nanoparticles: A paradigm shift in biomedical applications. Advances in colloid and interface science, 199-200, pp.44–58.

Khlebtsov, B.N., Khanadeev, V. a. & Khlebtsov, N.G., 2010. Attenuation, scattering, and depolarization of light by gold nanorods with silver shells. Optics and Spectroscopy, 108(1), pp.59–69.

Khlebtsov N.G. et al., 1996. Spectral Extinction of Colloidal Gold and Its Biospecific Conjugates. J. Colloid Interface Sci, 180(1), pp.436–445.

Khlebtsov, N.G. & Dykman, L.A., 2010. Optical properties and biomedical applications of plasmonic nanoparticles. JQSRT, 111(1), pp.1–35.

Kolwas, K. & Derkachova, A., 2013. Damping rates of surface plasmons for particles of size from nano- to micrometers; reduction of the nonradiative decay. JQSRT, 114, pp.45–55.

Kolwas, K. & Derkachova, A., 2010. Plasmonic abilities of gold and silver spherical nanoantennas in terms of size dependent multipolar resonance frequencies and plasmon damping rates. Opto-Electronics Review, 18(4), pp.429–437.

Kolwas, K, Derkachova, A. & Shopa, M., 2013. Practical tools for optimising plasmon enhanced near fields for optical diagnostic of molecules and cells. Journal of Biomaterials and Tissue Engeneering, pp.1–9, *in print*.

Kolwas, K., Derkachova, A. & Shopa, M., 2009. Size characteristics of surface plasmons and their manifestation in scattering properties of metal particles. JQSRT, 110(14-16), pp.1490–1501.

Kreibig, U. & Vollmer, M., 1995. Optical Properties of Metal Clusters Heidelber: Springer.

Lakowicz, J.R., 2006. Plasmonics in Biology and Plasmon-Controlled Fluorescence. Plasmonics (Norwell, Mass.), 1(1), pp.5–33.

Liao, H., Nehl, C.L. & Hafner, J.H., 2006. Biomedical applications of plasmon resonant metal nanoparticles. Nanomedicine, 1(2), pp.201–8.

Lin, H.-Y. et al., 2010. Direct near-field optical imaging of plasmonic resonances in metal nanoparticle pairs. Optics express, 18(1), pp.165–172.

Loo, C. et al., 2005. Immunotargeted nanoshells for integrated cancer imaging and therapy. Nano letters, 5(4), pp.709–711.

Maier, S.A. & Atwater, H.A., 2005. Plasmonics: Localization and guiding of electromagnetic energy in metal/dielectric structures. Journal of Applied Physics, 98(1), p.011101.

Mahajan, S. Et al., 2010. Understanding the Surface-Enhanced Raman Spectroscopy "Background". The Journal of Physical Chemistry C, 114(16), pp.7242–7250.

Oldenburg, S.J. et al., 1998. Nanoengineering of optical resonances, Chemical Physics Letters 288, pp. 243–247

Pradeep, T., 2009. Noble metal nanoparticles for water purification: A critical review. Thin Solid Films, 517(24), pp.6441–6478.

Quinten, M., 2011. Optical Properties of Nanoparticle Systems, Wiley-VCH Verlag GmbH & Co.

Rogobete, L. et al., 2007. Design of plasmonic nanoantennae for enhancing spontaneous emission. Optics Letters, 32(12), pp.1623–1625.

Sambles, J. & Bradbery, G., 1991. Optical excitation of surface plasmons: an introduction. Contemporary physics, 32(3), pp.173–183.

Sardar, R. et al., 2009. Gold nanoparticles: past, present, and future. Langmuir: the ACS journal of surfaces and colloids, 25(24), pp.13840–13851.

Schneider, T. et al., 2013. Localized surface plasmon resonance (LSPR) study of DNA hybridization at single nanoparticle transducers. Journal of Nanoparticle Research, 15(4), p.1531.

Schuller, J. A et al., 2010. Plasmonics for extreme light concentration and manipulation. Nature materials, 9(3), pp.193–204.

Shen, Y. et al., 2000. Nanophotonics: interactions, materials and applications. J. Phys. Chem. B, 104, pp.7577–7587.

Sönnichsen, C. et al., 2002. Plasmon resonances in large noble-metal clusters. New Journal of Physics, 4, pp.93–93.

Sönnichsen, C., 2001. Plasmons in metal nanostructures. Ludwig-Maximilians-Universität München. http://edoc.ub.uni-muenchen.de/2367/1/Soennichsen_Carsten.pdf.

Stuart, D. & Haes, A., 2005. Biological applications of localised surface plasmonic phenomenae. IEE Proc. Nanobiotechnol., 152(1), pp.13–32.

Turkevich, J., Garton, G. & Stevenson, P., 1954. The color of colloidal gold. Journal of Colloid Science, 9, Supplement 1, pp.26–35.

Wang, Y. et al., 2007. SERS opens a new way in aptasensor for protein recognition with high sensitivity and selectivity. Chemical communications (Cambridge, England), 48, pp.5220–5222.

Wang, Y., Plummer, E.W. & Kempa, K., 2011. Foundations of Plasmonics. In Advances in Physics. Taylor & Francis.

Wax, A. & Sokolov, K., 2009. Molecular imaging and darkfield microspectroscopy of live cells using gold plasmonic nanoparticles. Laser & Photonics Review, 3(1-2), pp.146–158.

Weiner, J., 2009. The physics of light transmission through subwavelength apertures and aperture arrays. Reports on Progress in Physics, 72(6), p.064401.

Willets, K. & Van Duyne, R., 2007. Localized surface plasmon resonance spectroscopy and sensing. Annu. Rev. Phys. Chem., 58, pp.267–297.

Yang, S.-M. et al., 2008. Synthesis and assembly of structured colloidal particles. J. Mater. Chem., 18(19), pp.2177–2190.

Ye, J. et al., 2009. Fabrication, characterization, and optical properties of gold nanobowl submonolayer structures. Langmuir, 25(3), pp.1822–1827.

Zakharian, A.R., Moloney, J. V & Mansuripur, M., 2007. Surface plasmon polaritons on metallic surfaces. Optics express, 15(1), pp.183–197.